arXiv:2309.04160v5 [cs.LG] 27 May 2024

PRISM: Leveraging Prototype Patient Representations with Feature-Missing-Aware Calibration for EHR Data Sparsity Mitigation

Yinghao Zhu[1,2], **Zixiang Wang**[2], **Long He**[3], **Shiyun Xie**[1],
Xiaochen Zheng[4], **Liantao Ma**[2,†], **Chengwei Pan**[1,†]
[1]Beihang University, Beijing, China
[2]Peking University, Beijing, China
[3]Tsinghua University, Beijing, China
[4]ETH Zürich, Zürich, Switzerland
zhuyinghao@buaa.edu.cn, pancw@buaa.edu.cn, malt@pku.edu.cn

Abstract

Electronic Health Records (EHRs) contain a wealth of patient data; however, the sparsity of EHRs data often presents significant challenges for predictive modeling. Conventional imputation methods inadequately distinguish between real and imputed data, leading to potential inaccuracies of patient representations. To address these issues, we introduce PRISM, a framework that indirectly imputes data by leveraging prototype representations of similar patients, thus ensuring compact representations that preserve patient information. PRISM also includes a feature confidence learner module, which evaluates the reliability of each feature considering missing statuses. Additionally, PRISM introduces a new patient similarity metric that accounts for feature confidence, avoiding overreliance on imprecise imputed values. Our extensive experiments on the MIMIC-III, MIMIC-IV, PhysioNet Challenge 2012, eICU datasets demonstrate PRISM's superior performance in predicting in-hospital mortality and 30-day readmission tasks, showcasing its effectiveness in handling EHR data sparsity. For the sake of reproducibility and further research, we have made the code publicly available at https://github.com/yhzhu99/PRISM.

1 Introduction

Electronic Health Records (EHR) have become indispensable in modern healthcare, offering a rich source of data that chronicles a patient's medical history. Over recent years, machine learning techniques have gained significant attention for their ability to leverage time-series EHR data, which represented as temporal sequences of high-dimensional clinical variables [1], can significantly inform and enhance clinical decision-making. Such applications range from predicting the survival risk of patients [2, 3] to forecasting early mortality outcomes [4, 5, 6, 7].

Working with time-series EHR data presents challenges due to its inherent sparsity. Factors such as data corruption [8], expensive examinations [9], and safety considerations [10] result in missing observations; for instance, not all indicators are captured during every patient visit [11]. Imputed values, while necessary, are not genuine reflections of a patient's condition and can introduce noise, diminishing model accuracy [12]. Given that most machine learning models cannot process NaN (Not a Number) inputs, this sparsity necessitates imputation, complicating EHR predictive modeling.

† Corresponding author.

Preprint. Under review.

While most existing works tackling EHR sparsity have tried to perform the imputation task directly on raw data, based on modeling the health status trajectory of the whole training set, this approach is similar to that of matrix completion methods, such as MICE [13], non-negative matrix factorization (NMF) [14], and compressed sensing [15]. However, they fail to capture the temporal interactions of longitudinal EHR data for each patient. Also, previous EHR-specific models with strategies of recalibrating patient representations based on attentive feature importance [16, 17] exhibit an issue of inadvertently prioritizing imputed features, potentially introducing inaccuracies [18]. Thus, addressing the sparsity in time-series EHR data requires a focus on capturing relevant feature representations across visits within a patient or among patients that are essential for predictive purposes. The primary objective is to discern and highlight crucial features while diminishing the impact of irrelevant, redundant, or missing ones.

Intuitively, incorporating knowledge from similar patients as an indirect method of imputation has the potential to enhance patient representations in the context of sparse EHR data. Such a knowledge-driven approach mirrors the real-world clinical reasoning processes, harnessing patterns observed in related patient cases [19]. Regarding the identifying similar patient process, however, existing models also face a significant limitation: they cannot distinguish between actual and imputed data [3, 12]. Consider two patients who have the same lab test feature value. For patient A, this value originates from the actual data, while for patient B, it is an imputed value. Current similarity metrics, whether they are L1, L2 distance, cosine similarity [20], handcrafted metrics [21], or learning-based methods [19], interpret these values identically. This results in a potentially misleading perception of similarity.

Given these insights, we are confronted with a pressing challenge: **How can we effectively mitigate the sparsity issue in EHR data caused by missing recorded features while ensuring a compact patient representation that preserves patient information? [22]**

To address this, we introduce `PRISM` that leverages prototype similar patients representations at the hidden state space. Unlike traditional direct imputation methods that imputes values based only raw data, `PRISM` learns refined patient representations according to prediction targets, serving as a more effective imputation strategy and thus mitigating the EHR data sparsity issue. Central to our approach is the feature-missing-aware calibration process in the proposed feature confidence learner module. It evaluates the reliability of each feature, considering its absence, the time since the last recorded visit, and the overall rate of missing data in the dataset. By emphasizing feature confidence, our newly designed patient similarity measure provides evaluations based not just on raw data values, but also on the varying confidence levels of each feature.

In healthcare, the absence of data can severely compromise confidence in a prognosis. Addressing and understanding the challenges of these missing features is of utmost importance. In light of this, `PRISM` seeks to bridge this gap. Our primary contributions are:

- **Methodologically,** we propose `PRISM`, a framework for learning prototype representations of similar patients, designed to mitigate EHR data sparsity. We design the feature confidence learner that evaluates and calibrates the reliability of each feature by examining its absence and associated confidence level. We also introduce the confidence-aware prototype patient learner with enhanced patient similarity measures that differentiates between varying feature confidence levels. Compared to existing SOTA baselines, i.e. GRASP [3] and M3Care [12], `PRISM` provides a refined feature calibration, and further missing-aware similarity measure helps to identify more related patient representation, with missing feature status elaborately taking into account.
- **Experimentally**, comprehensive experiments on four real-world datasets, MIMIC-III, MIMIC-IV, Challenge-2012, and eICU, focusing on in-hospital mortality and 30-day readmission prediction tasks, reveal that `PRISM` significantly improves the quality of patient representations against EHR data sparsity. `PRISM` outperforms the best-performing baseline model with relative improvements of 6.40%, 2.78%, 1.51% and 11.01% in mortality on AUPRC for four datasets. In terms of readmission task, `PRISM` obtains relative improvements of 1.38% and 1.63% on AUPRC for MIMIC-III and MIMIC-IV, respectively. Further ablation studies and detailed experimental analysis underline `PRISM`'s effectiveness, robustness, adaptability, and efficiency.

2 Related Work

In the realm of EHR data analysis, irregular sampling often leads to significant data sparsity, presenting substantial challenges in modeling. Previous methods on sparse EHR data predominantly fall under two categories: direct imputation in the raw data space and indirect imputation within the feature representation space.

2.1 Direct Imputation

Direct imputation methods aim to estimate missing features or incorporate missing information directly. Traditional matrix imputation techniques, such as MICE [13], non-negative matrix factorization (NMF) [14], compressed sensing [15], or naive zero, mean, or median imputation, rely on similar rows or columns to fill in missing data. However, these methods often operate under the assumption that patient visits are independent and features are missing at random. GRU-D [11] adopts a more targeted approach by introducing missing statuses into the GRU network. By utilizing time interval and missing mask information, GRU-D treats missing data as "Informative Missing". Extending these capabilities, ConCare [2] and AICare [17] first apply directly imputed EHR data, then incorporate multi-head self-attention mechanisms to refine feature embeddings. This ensures contextual relevance across diverse healthcare situations, regardless of data completeness.

2.2 Indirect Imputation

As demonstrated in GRASP [3] and M3Care [12], they emphasize the use of similar patient representations to derive meaningful information with the insight that the information observed from similar patients can be utilized as guidance for the current patient's prognosis [3]. However, accurately measuring patient similarity is intrinsically challenging, especially when features might be imputed with potentially misleading information. Many traditional works, such as [20] and [21], have resorted to fixed formulas like cosine similarity and Euclidean distance to gauge patient similarity. While these methods are straightforward, they often suffer from scalability and performance limitations. A more dynamic approach is seen in [19], which adopts metric learning with triplet loss. This technique focuses on learning the relative distances between patients, where distances have an inverse correlation with similarity scores.

However, a shared oversight across the aforementioned methods is the underestimation of the impact of missing features. This is evident both during the recalibration of features and when assessing patient similarities, as highlighted in the introduction and essential to tackle the EHR sparsity issue.

3 Problem Formulation

3.1 EHR Datasets Formulation

EHR datasets consist of a sequence of dynamic and static information for each patient. Assuming that there are F features in total, D dynamic features (e.g., lab tests and vital signs) and S static features (e.g., sex and age), where $F = D + S$, at every clinical visit t. The features recorded at visit t can be denoted as $\boldsymbol{x}_t \in \mathbb{R}^F, t = 1, 2, \cdots, T$, with total T visits. The dynamic feature information can be formulated as a 2-dimensional matrix $\boldsymbol{d} \in \mathbb{R}^{T \times D}$, along with static information denoted as 1-dimensional matrix $\boldsymbol{s} \in \mathbb{R}^S$. In addition, to differentiate between categorical and numerical variables within dynamic features, we employ one-hot encoding for categorical variables. Due to the inherent sparsity of EHR data, we incorporate feature missingness as inputs. At a global view, we define the missing representation, denoted as ρ_i, to be the presence rate of the i-th feature within the entire dataset. From a local view, the missing representation, $\tau_{i,t}$, signifies the time interval since the last recorded visit that contains the i-th feature up to the t-th visit.

3.2 Predictive Objective Formulation

Prediction objective is presented as a binary classification task. Given each patient's EHR data $\boldsymbol{X} = [\boldsymbol{x_1}, \boldsymbol{x_2}, \cdots, \boldsymbol{x_T}]^\top \in \mathbb{R}^{T \times F}$ and feature missing status $\{\rho, \tau\}$ as input, where each $\boldsymbol{x_t}$ consists of dynamic features and static features representation, the model attempts to predict the specific clinical outcome, denoted as y. The objective is formulated as $\hat{y} = \text{Model}(\boldsymbol{X}, \{\rho, \tau\})$. For the

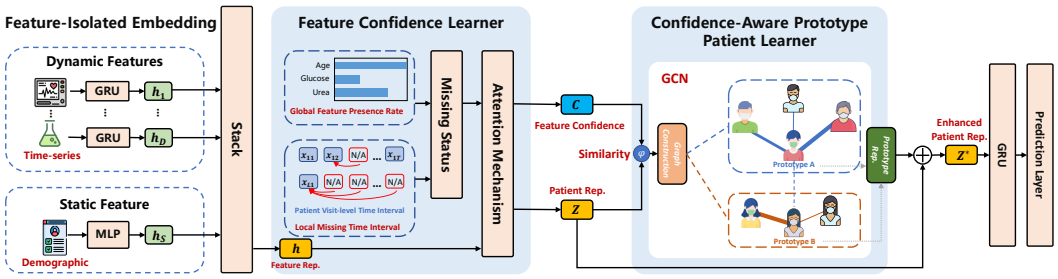

Figure 1: *Overall model architecture of our proposed method* `PRISM`. "Rep." means "Representation".

in-hospital mortality prediction task, the goal is to predict the discharge status (0 for alive, 1 for deceased) based on the initial 48-hour window of an ICU stay. Similarly, the 30-day readmission task predicts if a patient will be readmitted in 30 days (0 for no readmission, 1 for readmission).

3.3 Notation Table

Table 1 contains notation symbols and their descriptions used in the paper.

Table 1: *Notations symbols and their descriptions*

Notations	Descriptions
N	Number of patient samples
T	Number of visits for a certain patient
D	Number of dynamic features
S	Number of static features
F	Number of features, $F = S + D$
$\boldsymbol{d_{it}} \in \mathbb{R}^m$	The i-th feature at the t-th visit, where m is either the number of categories (for one-hot encoding) or 1 (for numerical lab tests)
$\boldsymbol{X} \in \mathbb{R}^{T \times F}$	Clinical visit matrix of a single patient, consisting of T visits
$\boldsymbol{s}, \boldsymbol{d}$	Static and dynamic feature vector of a patient
$\boldsymbol{y}, \hat{\boldsymbol{y}}$	Ground truth labels and prediction results
$\boldsymbol{h_i} \in \mathbb{R}^{T \times f}, \boldsymbol{h}$	Representation of i-th feature learned by GRU (for dynamic features) or MLP (for static features), stacked to form the representation matrix $\boldsymbol{h}$, f is each feature's embedding dimension
ρ_i	Feature presence rate of feature i in training set
$\tau_{i,t}$	Time interval from the last recorded visit of i-th feature at t-th visit
$\boldsymbol{C} \in \mathbb{R}^{T \times F}$	Learned feature confidence matrix of a patient
$\boldsymbol{z_i}$	$\boldsymbol{z_i}$ is the learned representation of the i-th patient after the feature calibration layer
$\boldsymbol{\alpha}, \boldsymbol{\alpha}^*$	Learned attention weights and calibrated attention weights after the feature calibration layer
$\phi(\cdot, \cdot)$	Patient similarity measure function
$\boldsymbol{A} = (a_{i,j})$	Adjacency matrix of patients, composed of similarity score between i-th and j-th patient
$\boldsymbol{\mathcal{G}_k}$	Learned prototype patient representation of the k-th group
$\boldsymbol{z_i^*}$	Learned representation of the i-th patient after representation fusion layer
$\boldsymbol{W}_\square$	Parameter matrices of linear layers. Footnote $\square$ denotes the name of the layer
K	Number of similar patient groups

4 Methodology

4.1 Overview

Figure 1 shows the overall pipeline of `PRISM`. It consists of three main sub-modules below.

- **Feature-Isolated Embedding Module** applies GRU and MLP backbone separately to dynamic features and static features. Each dynamic feature learns historical representations over multiple

time steps. To align with the original attribute information of each feature, the features are learned in isolation from each other.

- **Feature Confidence Learner** improves self-attention model by introducing the feature missing status (the global dataset-level and local patient-level missing representations of the features), collaboratively learning the confidence level of the features and the confidence-calibrated feature importance.
- **Confidence-Aware Prototype Patient Learner** improves the measure of patient similarity based on patient representation and the confidence level of features learned from feature missing status. It then applies the graph neural network to learn prototype patients. Finally, the patient's own representation is fused with the prototype patient representation adaptively, further enhancing the hidden state representation of the patient that is affected by missing data. A two-layer GRU network is then utilized to generate a compact patient health representation, followed by a single-layer MLP network to conduct downstream specific prediction tasks.

4.2 Feature-Isolated Embedding Module

In this module, static and dynamic features are learned individually via Multilayer Perceptron (MLP) and Gated Recurrent Unit (GRU) networks, yielding feature representations of unified dimensions f.

4.2.1 Static Features Embedding

Static features remain constant at each visit. Hence, we opt for a single-layer MLP for simplicity to map each static feature into the feature dimensions f:

$$\boldsymbol{h}_{\boldsymbol{s_i}} = \mathrm{MLP}_i(\boldsymbol{s_i}), \quad i = 1, 2, \cdots, S \tag{1}$$

where $\boldsymbol{s_i}$ is the i-th static feature. We employ S distinct-parameter MLPs for feature mappings.

4.2.2 Dynamic Features Embedding

To ensure that each feature's individual statistics, e.g. missing status can be incorporated with the corresponding feature, we adopt multi-channel GRU structure to avoid feature interaction at this stage. Each feature is embed with an isolated GRU, a time-series model that has a proven track record of consistent performance in EHR modeling [6]:

$$\boldsymbol{h}_{\boldsymbol{d_i}} = \mathrm{GRU}_i(\boldsymbol{d_i}), \quad i = 1, 2, \cdots, D \tag{2}$$

where GRU_i represents the GRU network applied to the i-th dynamic feature $\boldsymbol{d_i} \in \mathbb{R}^{T \times m}$. Furthermore, $\boldsymbol{h}_{\boldsymbol{d_i}} \in \mathbb{R}^{T \times f}$ signifies the embedding of the i-th dynamic feature. The in-channel of GRU is the feature recorded dimension m, and the out-channel is the unified f.

Then we employ a stack operation to integrate information from both static and dynamic features. This necessitates initially replicating the static features embeddings to each time visits: $\boldsymbol{h}_{\boldsymbol{s_i}} \in \mathbb{R}^f \rightarrow \boldsymbol{h'}_{\boldsymbol{s_i}} \in \mathbb{R}^{T \times f}$. The stack operation is represented as follows:

$$\boldsymbol{h} = \mathrm{stack}(\boldsymbol{h'}_{\boldsymbol{s_1}}, \boldsymbol{h'}_{\boldsymbol{s_2}}, \cdots, \boldsymbol{h'}_{\boldsymbol{s_S}}, \boldsymbol{h}_{\boldsymbol{d_1}}, \cdots, \boldsymbol{h}_{\boldsymbol{d_D}}) \tag{3}$$

where $\boldsymbol{h} \in \mathbb{R}^{F \times T \times f}$ represents the overall embeddings of features.

4.3 Feature Confidence Learner

Existing models adopt various ways to enhance patient representations to mitigate the noise introduced by processing sparse EHR data. However, these models often use imputed data and ignore the impact of feature missing status, thus reducing the credibility of the learned hidden representation. We design a measurement called "feature confidence", which represents the reliability of the input feature values for each patient and each visit. In addition, we have incorporated this measure into the self-attention mechanism as a recalibration module to elevate low-confidence features' attention.

4.3.1 Feature Missing Status Representation

We introduce ρ and τ to record feature missing status. Global missing representation ρ_i represents the presence rate of the i-th feature in the original dataset:

$$\rho_i = \frac{\text{total observations of } i\text{-th feature}}{\text{total visits of all patients}} \tag{4}$$

For example, if the dataset collects a total of 100 data records during the visits of all patients, but certain feature is only recorded two times, then the ρ for this feature is $\frac{2}{100} = 0.02$. Local missing representation $\tau_{i,t}$ represents the time interval since the last record of this feature at the current visit. There are two special cases: case 1) If the feature is recorded at the current visit, it is marked as 0; case 2) if the feature has never been recorded before the current visit, it is marked as infinity:

$$\tau_{i,t} = \begin{cases} 0 & \text{if case 1)} \\ \infty & \text{if case 2)} \\ t - t^* & \text{otherwise} \end{cases} \tag{5}$$

where t^* is the time of the last record of the i-th feature.

4.3.2 Missing-Aware Self-Attention

To calculate the feature confidence, we comprehensively consider the missing feature status in the dataset, including the global missing representation ρ and local missing representation τ, and integrate them into a self-attention mechanism module.

First, the $Query$ vector is computed from the hidden representation of the last time step T, while the Key and $Value$ vectors are computed from the hidden representations of all time steps:

$$q_{i,T} = \boldsymbol{W}_i^q \cdot h_{i,T} \tag{6}$$

$$k_{i,t} = \boldsymbol{W}_i^k \cdot h_{i,t} \tag{7}$$

$$v_{i,t} = \boldsymbol{W}_i^v \cdot h_{i,t} \tag{8}$$

where $q_{i,T}$, $k_{i,t}$, $v_{i,t}$ are the $Query$, Key, $Value$ vectors respectively, and $\boldsymbol{W}_i^q$, $\boldsymbol{W}_i^k$, $\boldsymbol{W}_i^v$ are the corresponding projection matrices. Following this, we compute the attention weights as follows:

$$\boldsymbol{\alpha}_{i,*,t} = softmax(\frac{q_{i,T}\boldsymbol{k}_{*,t}^\top}{\sqrt{d_k}}) \tag{9}$$

Subsequently, the feature confidence learner takes into account both feature missing status and attention weights to compute the feature confidence, which serves as an uncertainty reference when identifying similar patients in subsequent steps:

$$C_{i,t} = \begin{cases} \tanh\left(\frac{\alpha_{i,t}}{\omega_{i,t}}\right) & \text{if } \tau_{i,t} \neq \infty \\ \beta \cdot \rho_i & \text{if } \tau_{i,t} = \infty \end{cases} \tag{10}$$

where $\omega_{i,t}$ and $\alpha_{i,t}$ are defined as:

$$\omega_{i,t} = \gamma_i \cdot \log(e + (1 - \alpha_{i,t}) \cdot \tau_{i,t}) \tag{11}$$

$$\alpha_{i,t} = AvgPool(\boldsymbol{\alpha}_{i,*,t}) \tag{12}$$

Here, the global missing parameter β is a learnable parameter for global missing representation and the time-decay ratio γ_i is a feature-specific learnable parameter to reflect the influence of local missing representation as time interval increases. The calculation of feature confidence is divided into two scenarios:

- When the feature has been examined in previous visits, the authentic values of the same patient are often used to complete features. However, the feature confidence of imputed values for this feature should significantly diminish when:
  - time interval $\tau_{i,t}$ is large. As the time interval increases, the feature confidence will decay sharply.
  - the time-decay ratio γ_i is high. The higher the time-decay ratio, the more severe the decay of the feature confidence level, and only the most recent recorded data matters.
- Until the present visit, the examination of this specific feature has not been conducted. In this scenario, the imputed values are derived from other patients and the global missing representation ρ is selected to depict the feature confidence for the current patient.

Finally, based on feature confidence, we can obtain the calibrated attention weights $\boldsymbol{\alpha}^*$ and further hidden representations $\boldsymbol{z}$.

$$\boldsymbol{\alpha}^* = \epsilon \cdot \boldsymbol{\alpha} + (1 - \epsilon) \cdot \boldsymbol{C} \tag{13}$$

$$\boldsymbol{z} = \boldsymbol{\alpha}^* \boldsymbol{V} \tag{14}$$

where ϵ is a learnable parameter, $\boldsymbol{\alpha}$, $\boldsymbol{C}$, $\boldsymbol{\alpha}^*$, $\boldsymbol{V}$, $\boldsymbol{z} \in \mathbb{R}^{T \times F}$ are attention weights, feature confidence, calibrated attention weights, value vector and learned representation of the input patient.

4.4 Confidence-Aware Prototype Patient Learner

We incorporate feature confidence status into our confidence-aware module for identifying similar patient cohorts, accounting for the impact of missing features. Inspired by GRASP's [3] graph convolutional network (GCN) framework, we further compute and integrate the similarity score within the GCN, considering the individual patient's feature confidence to prioritize the selection of patients most similar to the subject patient.

4.4.1 Confidence-Aware Patient Similarity Measure

To find similar patients, we calculate the similarity between the current patient and others using the confidence-aware patient similarity measure, resulting in a similarity score matrix $\boldsymbol{A}$. Specifically, the similarity score $\phi_{i,j}(\boldsymbol{z}_i, \boldsymbol{z}_j; \boldsymbol{C}_i, \boldsymbol{C}_j)$ between the i-th and j-th ($i \neq j$) patients is defined as Equation 15. Note that when $i = j$, indicating the comparison of a patient with themselves, the similarity score is defined in $\phi_{i,j} = 1$.

$$\phi_{i,j} = \frac{1}{(1 - \zeta) \cdot \frac{1}{F}(\psi_{i,j}^{(z)}(\boldsymbol{z}_i, \boldsymbol{z}_j) + \zeta \cdot \psi_{i,j}^{(C)}(\boldsymbol{C}_i, \boldsymbol{C}_j))} \tag{15}$$

where $\psi_{i,j}^{(z)}(\boldsymbol{z}_i, \boldsymbol{z}_j)$ measures the similarity of the patients' representations, $\psi_{i,j}^{(C)}(\boldsymbol{C}_i, \boldsymbol{C}_j)$ measures the confidence level of the two patients in their respective feature representations, and ζ serves as learnable weight to balance the two. They are defined as follows respectively:

$$\psi_{i,j}^{(z)}(\boldsymbol{z}_i, \boldsymbol{z}_j) = ||\boldsymbol{z_i} - \boldsymbol{z_j}||_2^2 \tag{16}$$

$$\psi_{i,j}^{(C)}(\boldsymbol{C}_i, \boldsymbol{C}_j) = \sum_{k=1}^{F} \exp(1 - C_{i,k}) \cdot \exp(1 - C_{j,k}) \tag{17}$$

4.4.2 Prototype Patients Cohort Discovery

To compute the enhanced representations of similar patients, we design the prototype patients cohort discovery module by incorporating GCN's capability to learn relationships between graph nodes. Initially, we utilize the K-Means clustering algorithm to cluster raw patient representation (F recorded or imputed features) into K groups. Subsequently, we identify the center vectors of K clusters as the initial K prototypes $\boldsymbol{\mathcal{G}_k}, k = 1, 2, \cdots, K$. These prototypes vectors, along with the patient groups, form the nodes of a graph. We then calculate the edge weights for this graph using a predefined similarity measure, resulting in an adjacency matrix $\boldsymbol{A}$. As GCN learns across epochs, the graph structure dynamically evolves. Note that the feature confidence $\mathbf{C}$ of prototype patients is initially set to 1 for each feature. During the training phase, both $\boldsymbol{\mathcal{G}}$ and the corresponding $\mathbf{C}$ are adaptively adjusted. Consequently, the most similar and representative prototypes $\boldsymbol{\mathcal{G}}$ are identified, and samples within the clusters become more similar to each other. The process is illustrated as:

$$\boldsymbol{\mathcal{G}}^* = \mathrm{MLP}(\mathrm{GCN}(\mathrm{concat}(\boldsymbol{z}, \boldsymbol{\mathcal{G}}), \boldsymbol{A})) \tag{18}$$

where $\boldsymbol{\mathcal{G}}^*$ is the updated prototype representation by GCN and MLP.

4.4.3 Prototype Representation Fusion

Currently, there are two learned hidden representations, one is $\boldsymbol{z}$ obtained through the missing-aware self-attention module, and the other is $\boldsymbol{\mathcal{G}}$ obtained through the prototype similar patient cohort discovery module. Thus, the patient representation is fused as:

$$\boldsymbol{z_i^*} = \eta \cdot \boldsymbol{\mathcal{G}_i} + (1 - \eta) \cdot \boldsymbol{z_i} \tag{19}$$

where η is a learnable weight parameter, $\boldsymbol{\mathcal{G}_i}$ is the corresponding prototype of the i-th sample.

4.5 Prediction Layers

Finally, the fused representation $\boldsymbol{z}^*$ is expected to predict downstream tasks. We sequentially pass $\boldsymbol{z}^*$ through two-layer GRU and a single-layer MLP network to obtain the final prediction results $\hat{y}$:

$$\hat{\boldsymbol{y}} = \text{MLP}(\text{GRU}(\boldsymbol{z}^*)) \tag{20}$$

The BCE Loss is selected as the loss function for the binary mortality outcome prediction task:

$$\mathcal{L}(\hat{y}, y) = -\frac{1}{n}\sum_{i=1}^{n}(y_i \log(\hat{y}_i) + (1 - y_i)\log(1 - \hat{y}_i)) \tag{21}$$

where n is the number of patients within one batch, $\hat{y} \in [0, 1]$ is the predicted probability and y is the ground truth.

5 Experimental Setups

5.1 Benchmarked Real-World Datasets

We employ MIMIC-III, MIMIC-IV, PhysioNet Challenge 2012, and eICU datasets datasets for benchmarking. All 4 datasets are split into 70% training set, 10% validation set and 20% test set with stratified shuffle split strategy based on patients' end-stage mortality outcome. By default, we use the Last Observation Carried Forward (LOCF) imputation method [23].

1. **MIMIC-III** [24] (Medical Information Mart for Intensive Care) is a large, freely-available database comprising information such as demographics, vital sign measurements made at the bedside, laboratory test results, procedures, medications, caregiver notes, imaging reports, and mortality.
2. **MIMIC-IV** [25] as MIMIC-III dataset's subsequent iteration, stands as an evolved manifestation of the MIMIC-III database, encompassing data updates and partial table reconstructions. We extracted patient EHR data following [26].
3. **PhysioNet Challenge 2012** [27] (Challenge-2012) covers records from 12,000 adult ICU stays. The challenge is designed to promote the development of effective algorithms for predicting in-hospital mortality based on data from the first 48 hours of ICU admission. We utilize 35 lab test features and 5 demographic features in Challenge-2012 dataset.
4. **eICU** [28] is a large-scale, multi-center ICU database derived from over 200,000 ICU admissions across the United States between 2014 and 2015. 12 lab test features and 2 demographic features are adopted.

The statistics of datasets is in Table 2.

Table 2: *Statistics of datasets after preprocessing.* The proportion demonstrates the percentage of the label with value 1. $Out.$ denotes Mortality Outcome, $Re.$ denotes Readmission.

Dataset	**MIMIC-III**	**MIMIC-IV**	**Challenge-2012**	**eICU**
# Samples	41517	56888	4000	73386
Missing	69.87%	74.70%	84.68%	42.61%
Label$_{Out.}$	10.62%	9.55%	13.85%	8.32%
Label$_{Re.}$	14.74%	13.85%	/	/

5.2 Evaluation Metrics

We assess the binary classification performance using AUROC, AUPRC and F1. Here we emphasize AUPRC as the main metric due to it is informative when dealing with highly imbalanced and skewed datasets [29, 30] as shown in our selected datasets.

5.3 Baseline Models

We include imputation-based methods, EHR-specific models, and `PRISM` model with reduced modules as baseline models.

5.3.1 Imputation-based Methods

We include two imputation-based methods: MICE and GRU-D:

- MICE [13] addresses missing data in EHR through iterative imputation, with subsequent analysis using an LSTM model [31].
- GRU-D [11] incoporates both the last observed and global mean values in the GRU network. Additionally, GRU-D utilizes an exponential decay mechanism to manage the temporal dynamics of missing values.

5.3.2 EHR-specific Models

Following methods are specifically designed for EHR data and focus on personalized health status embeddings.

- RETAIN [1] is a hierarchical attention-based interpretable model. It attends the EHR data in a reverse time order so that recent clinical visits are likely to receive higher attention.
- AdaCare [16] is a GRU-based network that utilizes a multi-scale dilated convolutional module to capture the long and short-term historical variation.
- ConCare [2] utilizes multi-channel GRU with a time-aware attention mechanism to extract clinical features and re-encode the clinical information by capturing the interdependencies between features.
- GRASP [3] is a generic framework for healthcare models, which leverages the information extracted from patients with similar conditions to enhance the cohort representation learning results.
- M3Care [12] resolves the missing modality issue in EHR data by utilizing similar patients' existing modalities. However, it does not address the issue of missing features within available modalities.
- SAFARI [5] learns patient health representations by applying a clinical-fact-inspired, task-agnostic correlational sparsity prior to medical feature correlations, using a bi-level optimization process that involves both inter- and intra-group correlations.
- AICare [17] also includes a multi-channel feature extraction module and an adaptive feature importance recalibration module. It learns personalized health status embeddings with static and dynamic features.

5.3.3 Ablation Models

Ablation models include $\texttt{PRISM}_{\text{-proto.}}$ and $\texttt{PRISM}_{\text{-calib.}}$.

- $\texttt{PRISM}_{\text{-proto.}}$ removes the confidence-aware prototype similar patient learner and reserves the feature-missing-aware calibration process. We apply the patients hidden representation $\boldsymbol{z}$ for downstream GRU module.
- $\texttt{PRISM}_{\text{-calib.}}$ removes the feature confidence learner from the missing-feature-aware calibration process. As the confidence-aware prototype patient learner requires the feature confidence $\boldsymbol{C}$ as input, we set the $\boldsymbol{C} = 1$ for each feature.

5.4 Implementation Details

5.4.1 Hardware and Software Configuration

All runs are trained on a single Nvidia RTX 3090 GPU with CUDA 11.8. The server's system memory (RAM) size is 64GB. We implement the model in Python 3.11.4, PyTorch 2.0.1 [32], PyTorch Lightning 2.0.5 [33], and pyehr [34].

5.4.2 Model Training and Hyperparameters

AdamW [35] is employed with a batch size of 1024 patients. All models are trained for 50 epochs with an early stopping strategy based on AUPRC after 10 epochs without improvement. The learning rate $0.01, 0.001, 0.0001$ and hidden dimensions $64, 128$ are tuned using a grid search strategy on the validation set. The searched hyperparameter for PRISM is: 128 hidden dimensions, 0.001 learning rate, and 256 prototype patient cluster numbers. Performance is reported in the form of mean±std of 5

runs with random seeds $0, 1, 2, 3, 4$ for MIMIC-III and MIMIC-IV datasets, and apply bootstrapping on all test set samples 10 times for the Challenge-2012 and eICU datasets, following practices in AICare [17].

6 Experimental Results and Analysis

We conduct the in-hospital mortality and 30-day readmission prediction task on MIMIC-III and MIMIC-IV datasets, in-hospital mortality prediction task on Challenge-2012 and eICU datasets. The dataset preprocessing scripts, developed model's code and all baseline models' code are attached at the Supplementary Material for reproducibility.

6.1 Experimental Results

Table 3 depicts the performance evaluation of baseline methods, PRISM, and its reduced versions for ablation study on four datasets under two prediction tasks. Additionally, we conduct t-test based on the AUPRC metric, the PRISM's performance improvement against all models are all statistically significant with p-value < 0.01, which underscores that PRISM significantly outperforms all baseline models. Specifically, PRISM outperforms models focused solely on enhancing feature representations with attention mechanisms (like RETAIN, AdaCare, ConCare, AICare, SAFARI), by integrating missing feature status into these mechanisms for improved attention calibration and feature representation. It also exceeds models using similar patient information (such as GRASP, M3Care), showing the value of missing feature status in refining prototype patient representations for better performance. PRISM's advantage over GRU-D, which only considers local patient visit-based feature missing status, highlights the significance of a global perspective on overall feature missing rates for effective feature representation across patients.

Table 3: *Benchmarking results on MIMIC-III, MIMIC-IV, Challenge-2012, and eICU datasets.* **Bold** indicates the best performance. Performance is reported in the form of mean±std. All metric scores are multiplied by 100 for readability purposes.

Dataset	MIMIC-III Mortality		MIMIC-III Readmission		MIMIC-IV Mortality		MIMIC-IV Readmission		Challenge-2012 Mortality		eICU Mortality	
Metric	AUPRC(↑)	AUROC(↑)	AUPRC(↑)	AUROC(↑)	AUPRC(↑)	AUROC(↑)	AUPRC(↑)	AUROC(↑)	AUPRC(↑)	AUROC(↑)	AUPRC(↑)	AUROC(↑)
MICE	52.40±0.57	85.43±0.23	50.61±0.47	77.97±0.60	49.89±0.78	84.37±0.13	75.84±0.25	45.28±0.38	32.26±2.85	72.41±1.46	44.44±4.16	85.19±2.97
GRU-D	45.31±3.22	81.72±2.46	42.13±3.19	73.31±1.65	48.79±1.57	85.02±0.50	76.47±0.53	45.03±0.71	25.43±3.27	63.75±1.76	42.59±3.33	83.85±2.31
RETAIN	51.76±0.86	85.57±0.43	47.53±0.48	77.42±0.38	54.06±0.71	86.24±0.36	78.54±0.38	49.93±0.73	30.23±2.24	69.82±1.89	39.89±3.08	82.53±2.45
AdaCare	52.28±0.50	85.73±0.19	48.76±0.35	77.65±0.32	50.45±0.80	83.96±0.13	77.00±0.20	48.57±0.29	33.10±3.42	69.66±1.57	42.48±3.61	83.91±2.32
ConCare	51.45±0.76	86.18±0.14	47.45±0.96	77.74±0.32	49.97±1.08	85.41±0.40	77.47±0.19	47.17±0.84	30.24±3.00	70.19±2.54	44.40±4.35	85.05±2.93
GRASP	53.59±0.33	86.54±0.17	50.21±0.22	78.14±0.35	54.41±0.46	86.08±0.17	78.50±0.22	50.22±0.26	26.03±3.43	67.14±2.61	45.41±4.05	85.69±2.38
M3Care	51.68±1.03	86.23±0.42	49.00±0.71	78.00±0.55	52.95±0.71	84.90±0.37	77.31±0.42	49.22±0.69	32.63±2.54	73.26±1.67	44.95±4.32	85.44±2.56
SAFARI	45.92±1.01	85.10±0.24	45.59±0.35	77.01±0.21	46.58±0.55	46.58±0.55	76.05±0.38	44.78±0.69	28.94±3.16	70.67±1.76	35.26±3.59	80.10±2.40
AICare	51.37±0.70	85.40±0.48	47.06±1.16	76.23±0.84	49.76±0.86	84.62±0.28	76.07±0.43	45.88±1.12	23.99±2.48	67.35±2.20	42.80±3.79	84.26±2.64
PRISM$_{\text{-proto.}}$	55.52±0.34	87.28±0.11	51.17±0.25	78.66±0.22	55.76±0.90	**86.82±0.16**	79.12±0.44	50.75±0.65	30.92±2.95	68.87±2.61	50.03±3.97	**85.93±1.67**
PRISM$_{\text{-calib.}}$	56.16±0.42	87.33±0.22	49.13±2.11	77.87±0.88	55.18±0.77	86.57±0.20	78.66±0.45	50.62±0.70	30.42±2.96	71.07±2.13	46.92±3.20	84.69±1.39
PRISM	**57.02±0.38**	**87.34±0.22**	**51.31±1.02**	**78.76±0.59**	**55.92±0.75**	**86.82±0.20**	**79.14±0.33**	**51.04±0.70**	**33.60±3.41**	**73.47±1.11**	**50.41±3.63**	85.82±1.43

6.2 Ablation Study

6.2.1 Comparing with Reduced Versions

PRISM outperforms PRISM$_{\text{-proto.}}$ and PRISM$_{\text{-calib.}}$ on main metric AUPRC. This indicates that the two designed learners can enhance patient feature representations from different perspectives: the patient's individual health data utilized by the feature confidence learner based on the attention mechanism and the prototype similar patient representations utilized by the prototype similar patient learner.

6.2.2 Comparing with Internal Components

To deeply explore the impact of components within each module, we conduct experiments in Table 4, showing PRISM outperforms all baselines. The symbol ϕ denotes similarity measure, detailed in Equation 15. The term $\boldsymbol{z}$ alone indicates the use of L2 distance for patient similarity measure, whereas $\boldsymbol{z}, \boldsymbol{C}$ additionally incorporates feature confidence, enhancing the model's discriminative capability. Comparing the roles of various components within the feature confidence learner, the performance when considering both global feature missing rate ρ and local patient's time interval τ is higher than considering any single component, which illustrates the necessity of considering the feature missing status from both global and local perspectives. When only considering the local perspective,

its performance actually worsens, which is consistent with our observation of the performance of GRU-D. As for confidence-aware prototype patient learner, the performance of confidence-aware patient similarity measurement surpasses that without considering feature confidence, which also shows the impact of missing feature status on measuring similar patients.

Table 4: *Performance comparison of internal components on the MIMIC-IV mortality prediction task.* "Feat. Conf." means "Feature Confidence" and "Sim. Meas." denotes "Similarity Measure". **Bold** denotes the best performance within each components, **Red** denotes the highest performance among all comparisons. Performance is reported in the form of mean±std. All metric scores are multiplied by 100 for readability purposes.

Comparisons	Components			Metrics	
	$+\rho$	$+\tau$	$+\phi$	AUPRC(↑)	AUROC(↑)
Feat. Conf.	/	/	/	54.42±0.43	86.22±0.30
	√	/	/	55.11±0.53	86.56±0.33
	/	√	/	52.67±2.52	86.43±0.55
	√	√	/	**55.76±0.90**	**86.82±0.16**
Sim. Meas.	/	/	$\boldsymbol{z}$	55.18±0.77	86.57±0.20
	/	/	$\boldsymbol{z}, \boldsymbol{C}$	**55.25±0.75**	**86.60±0.19**
PRISM	√	√	$\boldsymbol{z}, \boldsymbol{C}$	**55.92±0.75**	**86.82±0.20**

6.3 Observations and Analysis

6.3.1 Robustness to Data Sparsity

To assess PRISM's performance under conditions of data sparsity, we compare it with leading models such as GRASP, MICE(LSTM), and RETAIN in MIMIC-IV in-hospital mortality prediction task. At the volume-level in Figure 2(a), we reduce the data samples in training set, while at the feature-level in Figure 2(b), we intentionally increase the missing feature rates beyond the original missing rate. PRISM excels in both settings. Notably, in situations of extreme data sparsity, such as using only 10% training data and with an overall 97.47% feature missing rate, PRISM significantly outperforms the other models, highlighting its robustness in handling sparse data.

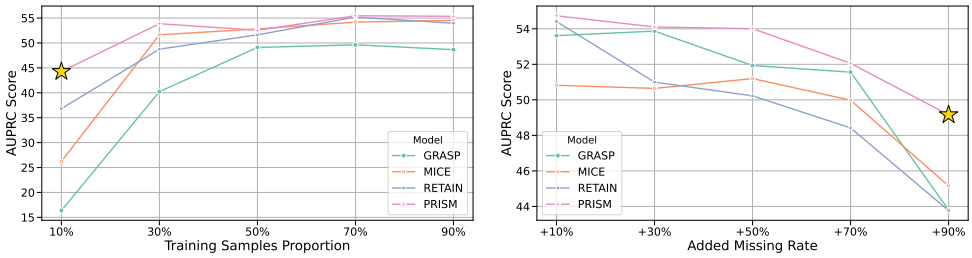

(a) Volume-level Sparsity (b) Feature-level Sparsity

Figure 2: *AUPRC performance across 5 sparsity levels in MIMIC-IV in-hospital mortality prediction task.* PRISM significantly outperforms other models in extremely sparse scenarios on both sparsity settings.

6.3.2 Sensitiveness to Cohort Size and Effectiveness of Missing-Feature-Aware Module

We conduct a detailed analysis to examine the impact of prototype patients cohort diversity and the role of a missing-feature-aware module in patient prototypes. Figure 3 shows that integrating a missing-feature-aware module consistently enhances performance across various cluster sizes, as indicated by the superior AUPRC and F1 score. Furthermore, the relatively consistent performance across different cluster sizes demonstrates that our model is not overly sensitive to the number of clusters, highlighting its adaptability and robustness in managing various cohort sizes.

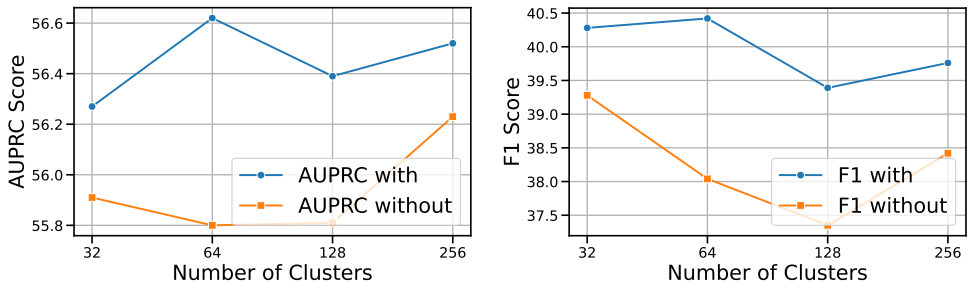

(a) AUPRC (b) F1

Figure 3: *AUPRC and F1 score performance on various prototype patient cohort size in MIMIC-IV in-hospital mortality prediction task.* With the missing-feature-aware module, PRISM outperforms its counterpart without. It also shows PRISM is not sensitive to the cohort size.

6.3.3 Variations of Similarity Measures

We assess the performance of PRISM by comparing it against standard similarity metrics commonly used in evaluating patient similarities. Table 5 details the results of this comparison on the MIMIC-IV in-hospital mortality prediction task. As demonstrated in the table, PRISM, leveraging a confidence-aware patient similarity measure, consistently surpasses traditional metrics such as cosine similarity, and L1 and L2 distances. This showcases the effectiveness of PRISM's similarity metric in measuring the impact of missing features.

Table 5: *Comparing different similarity measures in MIMIC-IV in-hospital mortality prediction task.* Performance is reported in the form of mean±std. All metric scores are multiplied by 100 for readability purposes.

Measure	**AUPRC**(↑)	**AUROC**(↑)	**F1**(↑)
Cosine	55.58±0.43	86.81±0.10	45.44±1.99
L1	55.59±0.54	86.73±0.20	45.20±1.91
L2	55.38±0.51	86.76±0.09	43.69±1.25
PRISM	**55.92±0.75**	**86.82±0.20**	**45.47±2.26**

6.3.4 Model Efficiency and Complexity

We evaluate the efficiency and complexity of PRISM against SOTA EHR-specific models baseline models. Table 6 compares the total parameter count and runtime of PRISM with these models on the MIMIC-IV dataset, using the same hidden dimension (128) and batch size (1024) hyperparameters. PRISM achieves a competitive balance between a low parameter count (215K) and an efficient runtime (69.03s).

Table 6: *Computational comparison with latest SOTA EHR-specific models on the MIMIC-IV dataset.* All models employ the same 128 hidden dimension and 1024 batch size hyperparameters.

Model	**# Parameter**	**Runtime (5 epochs)**
ConCare (AAAI-2020)	3.3M	96.62s
GRASP (AAAI-2021)	3.3M	97.68s
M3Care (KDD-2022)	469K	68.29s
SAFARI (TKDE-2022)	1.8M	78.97s
AICare (Patterns-2023)	2.2M	72.97s
PRISM	215K	69.03s

Table 7 presents the data preparation time for PRISM on MIMIC-III and MIMIC-IV datasets, including preprocessing, training, validation, and testing. The PRISM pipeline seamlessly computes feature

missing statuses in the LOCF pipeline with little extra cost. Moreover, the entire pipeline can be completed within 10 minutes for each dataset.

Table 7: *Data preparation time comparison.* Prep. denotes Preprocessing, Val. denotes Validation. All with 50 epochs of training, validate at the end of each epoch. The units are seconds.

Dataset	**MIMIC-III**			**MIMIC-IV**		
Prep.	w/o Impute	LOCF	+Ours	w/o Impute	LOCF	+Ours
Time	77.06	300.63	432.19	104.67	358.29	502.68
Pipeline	Data Prep.	Train+Val.	Test	Data Prep.	Train+Val.	Test
Time	432.19	505.83	10.25	502.68	510.73	12.39
Dataset	**Challenge-2012**			**eICU**		
Prep.	w/o Impute	LOCF	+Ours	w/o Impute	LOCF	+Ours
Time	18.46	56.59	85.14	52.99	146.54	170.21
Pipeline	Data Prep.	Train+Val.	Test	Data Prep.	Train+Val.	Test
Time	85.14	85.55	1.47	170.21	268.17	4.99

6.3.5 Cross-Feature Attention Map

Figure 4 presents the cross-feature attention map from PRISM, contrasting average attention weights with and without feature confidence calibration process. This visualization, based on a single diagnostic record from randomly selected MIMIC-IV patients, plots Key features on the x-axis against Query features on the y-axis. Notably, PRISM reduces attention on features like capillary refill rate, fraction inspired oxygen, and height, which have high missing rates (99.64%, 93.62%, and 99.61%, respectively) in the dataset. PRISM accurately recognizes and calibrates the features with high missing rates, thereby causing the three horizontal lines on the right side of the graph to appear distinctively whiter, showcasing attention-based feature learner module's interpretability which other baselines lack.

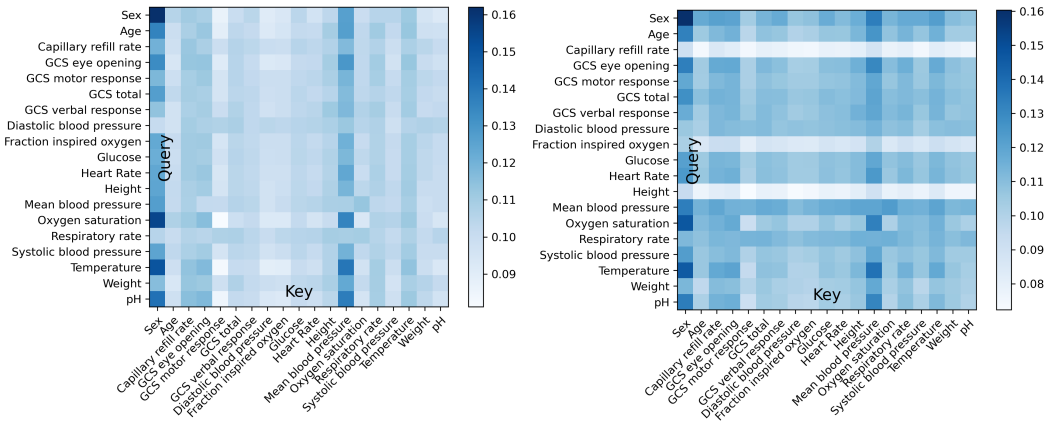

Figure 4: *Cross-feature attention maps from PRISM: Without (Left) / With (Right) feature confidence calibration.* The maps use data from a single MIMIC-IV patient record to show PRISM's reduction in attention to unreliable features (capillary refill rate, fraction inspired oxygen, height) due to high missing rates.

6.3.6 Patient Representation Visualization

To investigate the impact of the missing-feature-calibration process on the hidden representations of patient data, we apply t-SNE to project these representations onto a two-dimensional space using the test set of all patients from the MIMIC-IV dataset. Figure 5 illustrates the t-SNE embeddings of the

patient representations generated by PRISM, both with and without the application of the missing-feature-calibration process. The calibrated representations (Figure 5(b)) exhibit improved separation and compactness, particularly for patients with mortal outcomes, compared to the representations without calibration (Figure 5(a)). This observation suggests that the missing-feature-calibration process enables PRISM to learn more informative and discriminative representations of patient data by effectively handling missing features and capturing the underlying patterns and relationships within the data.

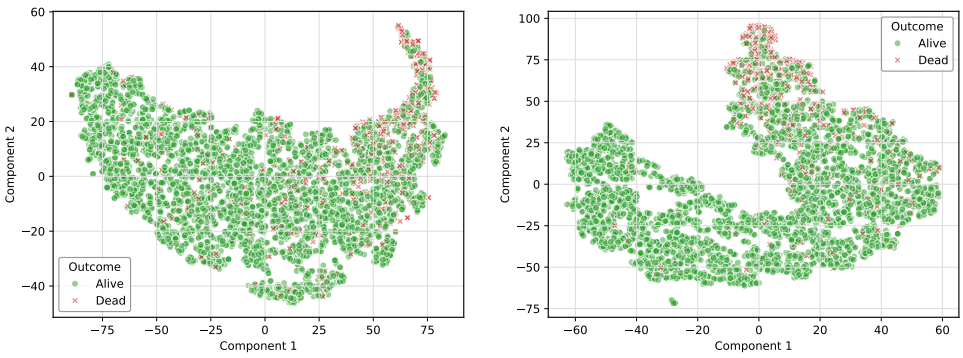

(a) Without calibration (b) With calibration

Figure 5: *t-SNE visualization of patient representations from PRISM.* (a) shows the embeddings without the missing-feature-calibration process, and (b) depicts embeddings with the process. (b)'s representations are more compact among dead outcome patients, showcasing it learns better representations.

6.3.7 Feature Decay Rates Observation

Figure 6 displays the decay rates of adaptive learning for various features, indicating how their importance diminishes over time. Higher decay rates suggest that the model prioritizes immediate changes in features like heart rate and pH, which is crucial for detecting acute medical conditions such as shock or infection. Conversely, features like sex and systolic blood pressure exhibit lower decay rates, highlighting their relevance in long-term analysis. Notice that the feature 'Height' exhibits short-term dynamics, likely due to being absent in over 99% of the data. Consequently, the rapid decay of the 'Height' feature, resulting from its high missing rate, does not significantly influence clinical decisions over the long term, which aligns with our intuition.

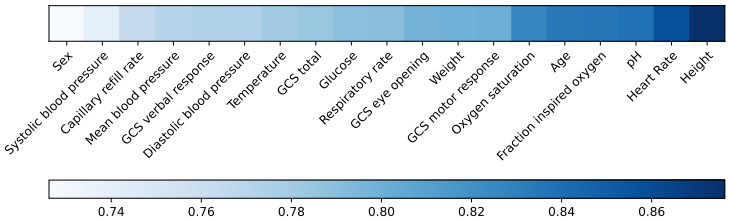

Figure 6: *Adaptive learning feature decay rates.* The graph shows varying decay rates: high for acute-indicator features like heart rate and pH, and low for longer-term relevant features like sex and systolic blood pressure.

7 Limitations and Further Work

We propose potential limitations of our current model and suggest directions for future research:

- **Fairness Concerns:** Like many machine learning applications, it is essential to evaluate our model's fairness across various demographic groups [7]. Discovering bias issue in similar patients cohort could be further explored.

- **Scalability Issues:** The proposed model's scalability to more massive datasets or integration within real-time healthcare systems is yet to be assessed.
- **Prototype Patient Representations:** Though leveraging prototype patient representations has shown promise, further work is needed to understand the diversity of these prototypes. More intricate mechanisms for prototype generation, beyond similarity metrics, could also be explored.

8 Conclusions

In this work, we propose PRISM, a prototype patient representation learning framework to address the sparsity issue of EHR data. PRISM perceives and calibrates for missing features, thereby refining patient representations via a confidence-aware prototype patient learner. Significant performance improvements and detailed experimental analysis on four real-world datasets' in-hospital mortality and 30-day readmission prediction tasks show PRISM's effectiveness. The work marks a crucial step towards more reliable and effective utilization of EHR data in healthcare, offering a potent solution to the prevalent issue of data sparsity in clinical decision-making.

Ethical Statement

This study, which involves analyzing Electronic Health Records (EHR) from the MIMIC-III, MIMIC-IV, PhysioNet Challenge 2012, and eICU datasets, is dedicated to maintaining high ethical standards. All datasets used are de-identified to ensure patient confidentiality and privacy. By signing the data use agreement, we reaffirm our commitment to responsible data handling and usage. Our methodology is designed to minimize potential harm and to produce findings that are as unbiased and equitable as possible, reflecting the diverse and complex nature of medical data. We have also taken rigorous steps to ensure that our research adheres to these ethical values.

References

[1] Edward Choi, Mohammad Taha Bahadori, Jimeng Sun, Joshua Kulas, Andy Schuetz, and Walter Stewart. Retain: An interpretable predictive model for healthcare using reverse time attention mechanism. *Advances in neural information processing systems*, 29, 2016.

[2] Liantao Ma, Chaohe Zhang, Yasha Wang, Wenjie Ruan, Jiangtao Wang, Wen Tang, Xinyu Ma, Xin Gao, and Junyi Gao. Concare: Personalized clinical feature embedding via capturing the healthcare context. *Proceedings of the AAAI Conference on Artificial Intelligence*, 34(01):833–840, Apr. 2020.

[3] Chaohe Zhang, Xin Gao, Liantao Ma, Yasha Wang, Jiangtao Wang, and Wen Tang. Grasp: Generic framework for health status representation learning based on incorporating knowledge from similar patients. *Proceedings of the AAAI Conference on Artificial Intelligence*, 35(1):715–723, May 2021.

[4] Li Yan, Hai-Tao Zhang, Jorge Goncalves, Yang Xiao, Maolin Wang, Yuqi Guo, Chuan Sun, Xiuchuan Tang, Liang Jing, Mingyang Zhang, et al. An interpretable mortality prediction model for covid-19 patients. *Nature machine intelligence*, 2(5):283–288, 2020.

[5] Xinyu Ma, Yasha Wang, Xu Chu, Liantao Ma, Wen Tang, Junfeng Zhao, Ye Yuan, and Guoren Wang. Patient health representation learning via correlational sparse prior of medical features. *IEEE Transactions on Knowledge and Data Engineering*, 2022.

[6] Junyi Gao, Yinghao Zhu, Wenqing Wang, Guiying Dong, Wen Tang, Hao Wang, Yasha Wang, Ewen M Harrison, and Liantao Ma. A comprehensive benchmark for covid-19 predictive modeling using electronic health records in intensive care. *Patterns*, 2024.

[7] Yinghao Zhu, Jingkun An, Enshen Zhou, Lu An, Junyi Gao, Hao Li, Haoran Feng, Bo Hou, Wen Tang, Chengwei Pan, and Liantao Ma. M3fair: Mitigating bias in healthcare data through multi-level and multi-sensitive-attribute reweighting method. *arXiv preprint arXiv:2306.04118*, 2023.

[8] Jiayi Chen and Aidong Zhang. Hgmf: heterogeneous graph-based fusion for multimodal data with incompleteness. In *Proceedings of the 26th ACM SIGKDD international conference on knowledge discovery & data mining*, pages 1295–1305, 2020.

[9] FM Ford and J Ford. Non-attendance for social security medical examination: patients who cannot afford to get better? *Occupational medicine*, 50(7):504–507, 2000.

[10] Tao Zhou, Huazhu Fu, Geng Chen, Jianbing Shen, and Ling Shao. Hi-net: hybrid-fusion network for multi-modal mr image synthesis. *IEEE transactions on medical imaging*, 39(9):2772–2781, 2020.

[11] Zhengping Che, Sanjay Purushotham, Kyunghyun Cho, David Sontag, and Yan Liu. Recurrent neural networks for multivariate time series with missing values. *Scientific reports*, 8(1):6085, 2018.

[12] Chaohe Zhang, Xu Chu, Liantao Ma, Yinghao Zhu, Yasha Wang, Jiangtao Wang, and Junfeng Zhao. M3care: Learning with missing modalities in multimodal healthcare data. In *Proceedings of the 28th ACM SIGKDD Conference on Knowledge Discovery and Data Mining*, KDD '22, page 2418–2428, New York, NY, USA, 2022. Association for Computing Machinery.

[13] Stef Van Buuren and Karin Groothuis-Oudshoorn. mice: Multivariate imputation by chained equations in r. *Journal of statistical software*, 45:1–67, 2011.

[14] Yu-Xiong Wang and Yu-Jin Zhang. Nonnegative matrix factorization: A comprehensive review. *IEEE Transactions on knowledge and data engineering*, 25(6):1336–1353, 2012.

[15] Miles Lopes. Estimating unknown sparsity in compressed sensing. In *International Conference on Machine Learning*, pages 217–225. PMLR, 2013.

[16] Liantao Ma, Junyi Gao, Yasha Wang, Chaohe Zhang, Jiangtao Wang, Wenjie Ruan, Wen Tang, Xin Gao, and Xinyu Ma. Adacare: Explainable clinical health status representation learning via scale-adaptive feature extraction and recalibration. *Proceedings of the AAAI Conference on Artificial Intelligence*, 34(01):825–832, Apr. 2020.

[17] Liantao Ma, Chaohe Zhang, Junyi Gao, Xianfeng Jiao, Zhihao Yu, Yinghao Zhu, Tianlong Wang, Xinyu Ma, Yasha Wang, Wen Tang, Xinju Zhao, Wenjie Ruan, and Tao Wang. Mortality prediction with adaptive feature importance recalibration for peritoneal dialysis patients. *Patterns*, 4(12), 2023.

[18] Mingxuan Liu, Siqi Li, Han Yuan, Marcus Eng Hock Ong, Yilin Ning, Feng Xie, Seyed Ehsan Saffari, Yuqing Shang, Victor Volovici, Bibhas Chakraborty, et al. Handling missing values in healthcare data: A systematic review of deep learning-based imputation techniques. *Artificial Intelligence in Medicine*, page 102587, 2023.

[19] Qiuling Suo, Fenglong Ma, Ye Yuan, Mengdi Huai, Weida Zhong, Jing Gao, and Aidong Zhang. Deep patient similarity learning for personalized healthcare. *IEEE Transactions on NanoBioscience*, page 219–227, Jul 2018.

[20] Joon Lee, David M. Maslove, and Joel A. Dubin. Personalized mortality prediction driven by electronic medical data and a patient similarity metric. *PLOS ONE*, 10(5):e0127428, May 2015.

[21] Yanqun Huang, Ni Wang, Honglei Liu, Hui Zhang, Xiaolu Fei, Lan Wei, and Hui Chen. Study on patient similarity measurement based on electronic medical records. *Studies in health technology and informatics,Studies in health technology and informatics*, Aug 2019.

[22] Yuqi Si, Jingcheng Du, Zhao Li, Xiaoqian Jiang, Timothy Miller, Fei Wang, W Jim Zheng, and Kirk Roberts. Deep representation learning of patient data from electronic health records (ehr): A systematic review. *Journal of biomedical informatics*, 115:103671, 2021.

[23] Stephen B Woolley, Alex A Cardoni, and John W Goethe. Last-observation-carried-forward imputation method in clinical efficacy trials: review of 352 antidepressant studies. *Pharmacotherapy: The Journal of Human Pharmacology and Drug Therapy*, 29(12):1408–1416, 2009.

[24] Alistair EW Johnson, Tom J Pollard, Lu Shen, Li-wei H Lehman, Mengling Feng, Mohammad Ghassemi, Benjamin Moody, Peter Szolovits, Leo Anthony Celi, and Roger G Mark. Mimic-iii, a freely accessible critical care database. *Scientific data*, 3(1):1–9, 2016.

[25] Alistair EW Johnson, Lucas Bulgarelli, Lu Shen, Alvin Gayles, Ayad Shammout, Steven Horng, Tom J Pollard, Sicheng Hao, Benjamin Moody, Brian Gow, et al. Mimic-iv, a freely accessible electronic health record dataset. *Scientific data*, 10(1):1, 2023.

[26] Hrayr Harutyunyan, Hrant Khachatrian, David C Kale, Greg Ver Steeg, and Aram Galstyan. Multitask learning and benchmarking with clinical time series data. *Scientific data*, 6(1):96, 2019.

[27] Ikaro Silva, George Moody, Daniel J Scott, Leo A Celi, and Roger G Mark. Predicting in-hospital mortality of icu patients: The physionet/computing in cardiology challenge 2012. In *2012 Computing in Cardiology*, pages 245–248. IEEE, 2012.

[28] Tom J Pollard, Alistair EW Johnson, Jesse D Raffa, Leo A Celi, Roger G Mark, and Omar Badawi. The eicu collaborative research database, a freely available multi-center database for critical care research. *Scientific data*, 5(1):1–13, 2018.

[29] Misuk Kim and Kyu-Baek Hwang. An empirical evaluation of sampling methods for the classification of imbalanced data. *PLoS One*, 17(7):e0271260, 2022.

[30] Jesse Davis and Mark Goadrich. The relationship between precision-recall and roc curves. In *Proceedings of the 23rd international conference on Machine learning*, pages 233–240, 2006.

[31] Sepp Hochreiter and Jürgen Schmidhuber. Long short-term memory. *Neural computation*, 9(8):1735–1780, 1997.

[32] Adam Paszke, Sam Gross, Francisco Massa, Adam Lerer, James Bradbury, Gregory Chanan, Trevor Killeen, Zeming Lin, Natalia Gimelshein, Luca Antiga, et al. Pytorch: An imperative style, high-performance deep learning library. *Advances in neural information processing systems*, 32, 2019.

[33] William A Falcon. Pytorch lightning. *GitHub*, 3, 2019.

[34] Yinghao Zhu, Wenqing Wang, Junyi Gao, and Liantao Ma. Pyehr: A predictive modeling toolkit for electronic health records. https://github.com/yhzhu99/pyehr, 2024.

[35] Ilya Loshchilov and Frank Hutter. Decoupled weight decay regularization. *arXiv preprint arXiv:1711.05101*, 2017.